

# Multi-mode photonic crystal fibers for VCSEL based data transmission

N. A. Mortensen,<sup>1\*</sup> M. Stach,<sup>2</sup> J. Broeng,<sup>1</sup> A. Petersson,<sup>1</sup>  
H. R. Simonsen,<sup>1</sup> and R. Michalzik<sup>2</sup>

<sup>1</sup>Crystal Fibre A/S, Blokken 84, DK-3460 Birkerød, Denmark

<sup>2</sup>University of Ulm, Optoelectronics Department,  
Albert-Einstein-Allee 45, D-89069 Ulm, Germany

\*nam@crystal-fibre.com

**Abstract:** Quasi error-free 10 Gbit/s data transmission is demonstrated over a novel type of 50  $\mu\text{m}$  core diameter photonic crystal fiber with as much as 100 m length. Combined with 850 nm VCSEL sources, this fiber is an attractive alternative to graded-index multi-mode fibers for datacom applications. A comparison to numerical simulations suggests that the high bit-rate may be partly explained by inter-modal diffusion.

© 2018 Optical Society of America

**OCIS codes:** (060.2280) Fiber design and fabrication, (060.2330) Fiber optics communications, (999.999) Photonic crystal fiber

---

## References and links

1. R. Michalzik, K. J. Ebeling, M. Kicherer, F. Mederer, R. King, H. Unold, and R. Jager, "High-performance VCSELs for optical data links," IEICE T. Electron. **E84C**, 629 (2001).
2. P. Russell, "Review: Photonic Crystal Fibers," Science **299**, 358 (2003).
3. G. P. Agrawal, *Fiber-Optic Communication Systems* (Wiley & Sons, New York, 1997).
4. R. Michalzik, F. Mederer, H. Roscher, M. Stach, H. Unold, D. Wiedenmann, R. King, M. Grabherr, and E. Kube, "Design and communication applications of short-wavelength VCSELs," Proc. SPIE **4905**, 310 (2002).
5. S. G. Johnson and J. D. Joannopoulos, "Block-iterative frequency-domain methods for Maxwell's equations in a planewave basis," Opt. Express **8**, 173 (2001), <http://www.opticsexpress.org/abstract.cfm?URI=OPEX-8-3-173>
6. J. Lægsgaard, A. Bjarklev, and S. E. B. Libori, "Chromatic dispersion in photonic crystal fibers: fast and accurate scheme for calculation," J. Opt. Soc. Am. B **20**, 443 (2003).
7. A. K. Ghatak and K. Thyagarajan, *Introduction to Fiber Optics* (Cambridge University Press, Cambridge, 1998).

---

## 1 Introduction

Optical datacom as employed for the high-speed interconnection of electronic subsystems has rapidly gained importance over the past years. Vertical-cavity surface-emitting lasers (VCSELs) emitting in the 850 nm wavelength regime and simple step-index fibers or graded-index fibers are preferred key components for low-cost link solutions [1]. Whereas, due to strong inter-modal dispersion, the use of the former fiber type is limited to link lengths of some meters at Gbit/s data rates, fabrication of the latter requires supreme control over the refractive index profile, especially in optimized 50  $\mu\text{m}$  core diameter fibers enabling up to 300 m serial transmission of 10 Gbit/s signals. Since optical interconnect requirements move toward higher speed over shorter distances, the availability of an easily manufacturable, yet high-speed capable fiber medium would be very beneficial. In this paper, we report on the properties of a new type of multi-mode photonic crystal fiber (PCF) with relatively simple waveguide geometry and demonstrate 850 nm data transmission at 10 Gbit/s over a length of  $L = 100$  m. For a recent review of photonic crystal fibers we refer to Ref. [2] and references therein.

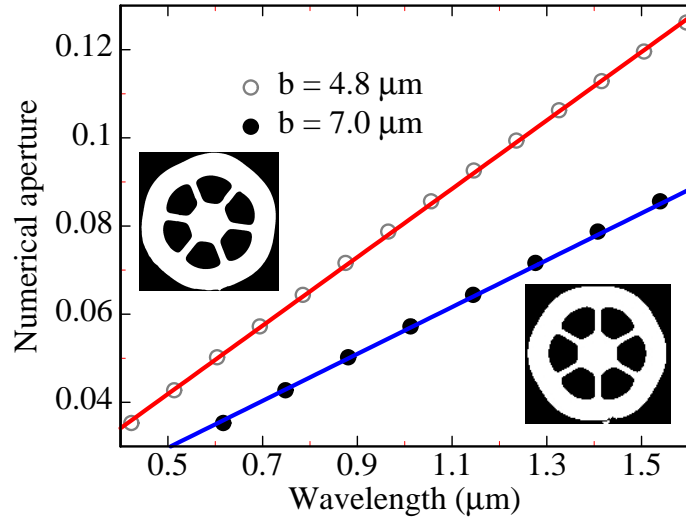


Fig. 1. Simulated NA for the  $33\text{ }\mu\text{m}$  core PCF (upper left inset) with bridges of width  $b \simeq 4.8\text{ }\mu\text{m}$  and the  $50\text{ }\mu\text{m}$  core PCF (lower right inset) with bridges of width  $b \simeq 7.0\text{ }\mu\text{m}$ . Note the different scale for the two insets.

## 2 Fiber design

The design of the new multi-mode photonic crystal fiber is illustrated in the insets of Fig. 1 which show optical micrographs of the fiber cross-sections. The fibers are made from a single material (light regions), and they comprise a solid, pure silica core suspended in air (dark regions) by narrow silica bridges of width  $b$ .

There is a large degree of freedom in engineering the optical properties and still get fiber designs of practical interest from a fabrication point of view. The properties may be tailored by adjusting parameters such as the size and shape of the core, the dimensions and number of silica bridges, or the fiber material. The numerical aperture (NA) of this type of PCF is essentially determined by the width of the silica bridges relative to the wavelength  $\lambda$  as numerically demonstrated in Fig. 1. Here, we focus on two fibers with  $33\text{ }\mu\text{m}$  and  $50\text{ }\mu\text{m}$  core diameter and bridge widths of  $b = 4.8\text{ }\mu\text{m}$  and  $7.0\text{ }\mu\text{m}$ , respectively, yielding NAs of around 0.07 and 0.05 at a wavelength of  $850\text{ nm}$ .

Despite the zero-index step between the core and the bridges, the fiber is capable of guiding light with good confinement to the multi-mode core. This is illustrated by the near-field intensity distributions for both the  $33\text{ }\mu\text{m}$  core PCF (Fig. 6) as well as the  $50\text{ }\mu\text{m}$  core PCF (the inset in Fig. 7).

We find that the fibers can be cleaved and spliced with commercially available equipment and typically, the fibers have an attenuation of the order  $50\text{ dB/km}$  at  $850\text{ nm}$  for typical bending radii such as  $16\text{ cm}$ .

## 3 Transmission experiments

Assuming worst-case conditions [3], we estimate from the above NA-values a bit rate-length product of around  $350\text{ MBit/s} \times \text{km}$  for the  $50\text{ }\mu\text{m}$  fiber, whereas the  $33\text{ }\mu\text{m}$  sample should have around  $180\text{ MBit/s} \times \text{km}$ . In what follows we examine the transmission properties of such PCFs with a length of  $L = 100\text{ m}$ .

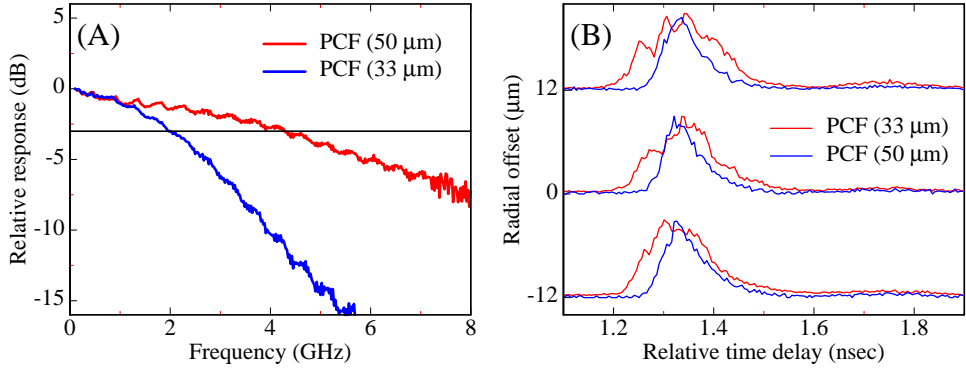


Fig. 2. Panel (A) shows small-signal frequency responses at 850 nm for a length  $L = 100$  m for the two PCFs illustrated in Fig. 1. Panel (B) shows normalized DMD plots for both fibers at offset positions of  $-12$ ,  $0$ , and  $12$   $\mu$ m.

### 3.1 Small-signal transfer function and DMD

In order to get a first indication of the fibers' expected transmission bandwidths, we have determined the small-signal frequency responses with a scalar network analyzer. As optical source, standard 850 nm GaAs based VCSELs have been employed. The  $12$   $\mu$ m active diameter, oxide-confined devices show transverse multi-mode emission with a root mean square spectral width of less than  $0.4$  nm even under modulation. The lasing threshold current amounts to  $1.8$  mA and the bias current for the small-signal as well as data transmission experiments was chosen as  $9$  mA, where the 3-dB bandwidth is  $8.6$  GHz. At the receiving end, a multi-mode fiber pigtailed InGaAs pin-photo-receiver with above  $8$  GHz bandwidth was used.

Panel (A) of Fig. 2 depicts the relative responses of both PCF samples. The  $33$  and  $50$   $\mu$ m core PCFs show a bit rate-length product of  $B_T \times L \sim 500$  Mbit/s  $\times$  km and  $\sim 1000$  Mbit/s  $\times$  km, respectively. These figures are significantly larger than expected from the corresponding NAs. In the next section we extend the NA estimations and show simulations of the modal time delays for the two PCFs.

In order to get quantitative insight into the modal delay properties, we have determined the PCFs differential mode delay (DMD) characteristics, see Panel (B) of Fig. 2. Here, a  $5$   $\mu$ m core diameter single-mode fiber is scanned over the PCF input at a distance of about  $10$   $\mu$ m in accordance with the IEC pre-standard 60793-1-49, Sect. 3.3. The impulse response at the output end is recorded for each offset position using an

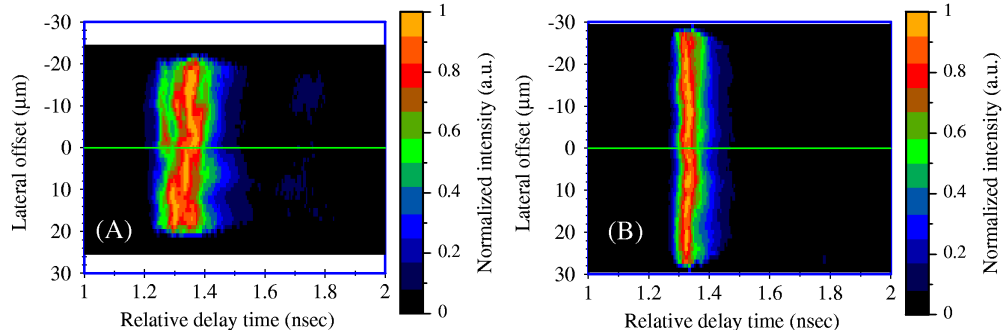


Fig. 3. Normalized DMD plots at variable offset positions. Panels (A) and (B) show results for the  $33$   $\mu$ m and the  $50$   $\mu$ m PCFs, respectively.

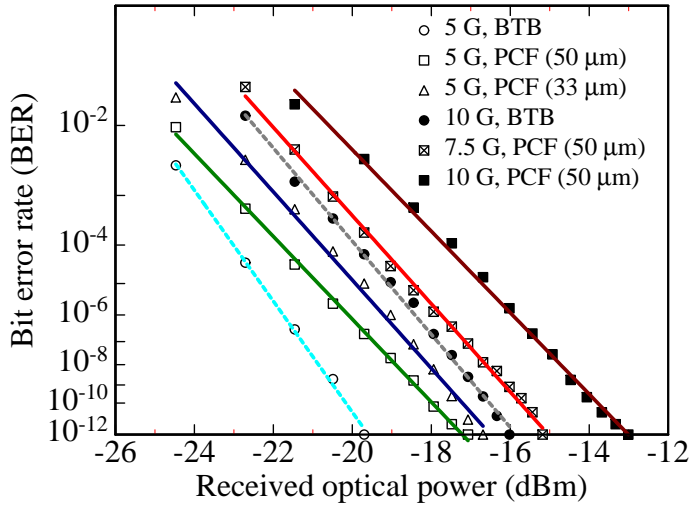


Fig. 4. BER characteristics for both 100 m-long PCFs at data rates of 5, 7.5, and 10 Gbit/s.

optical sampling oscilloscope with a fiber input compatible to  $62.5 \mu\text{m}$  core diameter multi-mode fibers. A gain-switched 850 nm single-mode VCSEL delivering pulses with less than 40 ps full width at half maximum is employed for this purpose [4]. Panel (B) illustrates some of the results. It is seen that the output pulses of the  $50 \mu\text{m}$  fiber are rather narrow and virtually independent of the offset position. On the other hand, those of the  $33 \mu\text{m}$  sample show larger variability and are up to twice as broad, which well supports the above observations. Figure 3 shows two-dimensional color-coded representations of the full data.

### 3.2 Digital data transmission

Data transmission experiments have been carried out under non-return-to-zero  $2^7 - 1$  word length pseudo-random bit sequence modulation using the aforementioned multi-mode VCSEL driven with 0.9 V peak-to-peak voltage. Figure 4 summarizes obtained bit error rate (BER) curves. With the smaller core diameter fiber, up to 5 Gbit/s could be transmitted without indication of a BER floor. The power penalty versus back-to-back (BTB) operation is about 3 dB at a BER of  $10^{-12}$ . On the other hand, the  $50 \mu\text{m}$  fiber even enables 10 Gbit/s transmission over  $L = 100$  m length with only 2.9 dB power penalty. The observed increase in data rate is in full agreement with the small-signal and DMD measurement results.

## 4 Simulations

We use a plane-wave method [5] to calculate the propagation constant  $\beta_m = n_m \omega / c$  of the  $m$ th eigenmode where  $n_m$  is the effective index,  $\omega$  the angular frequency, and  $c$  the vacuum velocity of light. For the refractive index profile we use optical micrographs transformed to one-bit format representing the two-component composite air-silica structure and for the refractive index we use a Sellmeier expression for  $n(\omega)$  in silica and  $n = 1$  in air. The simulation of Maxwell's equations for a given  $\omega$  provides us with sets of propagation constants  $\{\beta_m\}$  and eigenfields  $\{\mathbf{E}_m\}$  where  $m = 1, 2, 3, \dots, M$  with  $M$  as the number of guided eigenmodes. We determine  $M$  from the experimentally measured NA which we transform to an effective cladding index  $n_{\text{cl}}$ . The number of

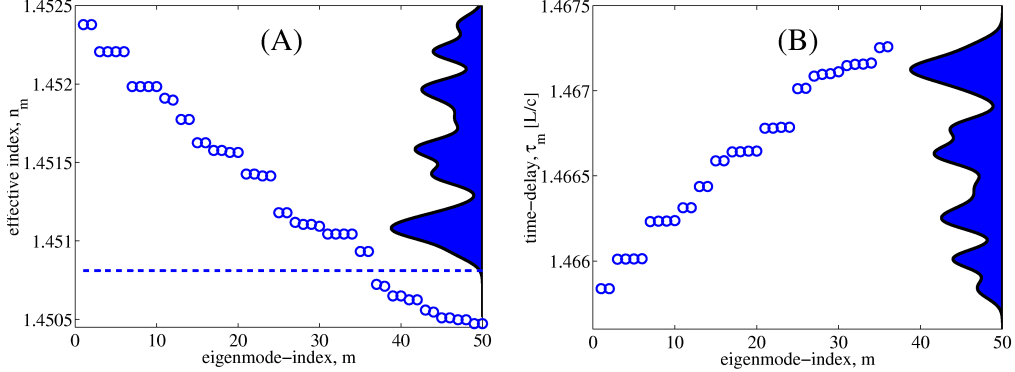


Fig. 5. Panel (A) shows the effective indices of the  $M = 36$  guided eigenmodes at  $\lambda = 850$  nm in the  $33 \mu\text{m}$  core PCF (see upper left inset of Fig. 1). The horizontal dashed line indicates the cladding index  $n_{cl}$  corresponding to the experimentally measured NA. The filled curve shows the distribution  $P(n_m)$  (the projection of the data onto the  $y$ -axis). Panel (B) shows the corresponding time-delays  $\tau_m$  and the distribution  $P(\tau_m)$ .

guided eigenmodes  $M$  then follows from the requirement that  $n_M > n_{cl} \geq n_{M+1}$ .

The delay-times (or group-delays) are given by  $\tau_m = L \partial \beta_m / \partial \omega$  (we calculate the group velocity by the approach described in Ref. [6]). The variation with  $m$  usually sets the limit on the bit rate and in that case the bit rate-length product is given by [3, 7]

$$B_T \times L \simeq L / \Delta T, \quad \Delta T \approx 2 \sqrt{\langle \{\delta^2 \tau_m\} \rangle}, \quad \delta \tau_m = \tau_m - \langle \{\tau_m\} \rangle, \quad (1)$$

Here, we use the second moment calculated from the full statistics to characterize the width  $\Delta T$  of the distribution  $P(\tau_m)$ . For the estimate of the bit-rate the eigenmodes are thus weighted equally corresponding to an assumption of uniform launch and attenuation. In literature one often finds the estimate  $\Delta T \approx \max\{\tau_m\} - \min\{\tau_m\}$  [3, 7] and in the ray-optical picture  $\max\{\tau_m\}$  can be expressed in terms of the NA in analogy to our estimations in section 3 based on the NA. However, for a sufficiently low number of guided modes the beginning break-down of geometrical optics calls for estimates based on the full statistics.

Figure 5 shows results at  $\lambda = 850$  nm for the  $33 \mu\text{m}$  core PCF (see upper left inset in Fig. 1). Experimentally, this fiber is found to have an NA  $\simeq 0.07$  and the corresponding effective cladding index is indicated by the dashed line in panel (A). For the given core size this results in  $M = 36$  eigenmodes that are guided. Panel (B) shows the results for the time-delays with the filled curve showing the distribution  $P(\tau_m)$  (the projection of the data onto the  $y$ -axis) calculated from a superposition of Gaussians with a width given by the mean level spacing  $(\tau_M - \tau_1)/(M - 1)$ . We have  $\Delta T \simeq 0.00087 \times L/c$  corresponding to  $B_T \times L \simeq 344 \text{ MBit/s} \times \text{km}$  which as expected is somewhat larger than the NA-estimate. The experimentally observed value is approximately 50% larger. It is wellknown that both non-uniform loss and attenuation as well as inter-modal diffusion tends to narrow the spread in time-delays. The DMD plots in Fig. 3 supports the presence of inter-modal diffusion and its dominance over both the excitation conditions as well as variations in modal attenuation. It is thus likely that the enhanced bit-rate length product originates from inter-modal diffusion. One could speculate that stress could modify the index-profile in the silica core and that this in turn could modify the time-delay

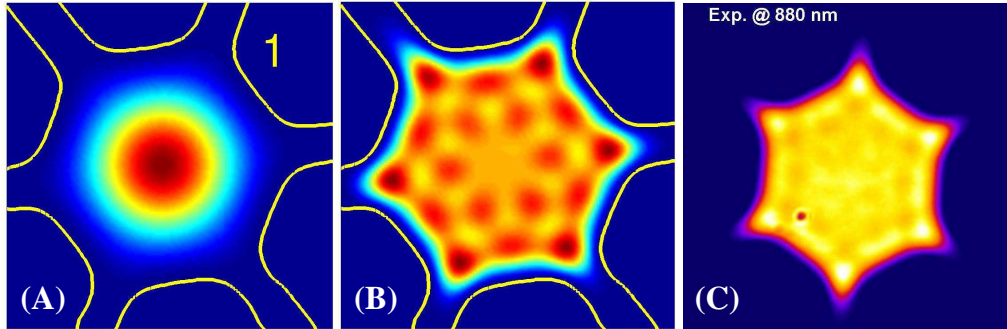


Fig. 6. Intensity distributions at  $\lambda = 850$  nm in the  $33\ \mu\text{m}$  PCF (see upper left inset in Fig. 1). Panel (A) shows the first ( $m = 1$ ) eigenmode (see <http://asger.hjem.wanadoo.dk/mm.gif> to view the other  $M = 36$  guided eigenmodes, 700 Kbyte). Panel (B) shows the average eigenfield intensity which agrees well with the experimentally observed near-field intensity shown in Panel (C). In Panels (A) and (B) the contour lines indicate the air-silica interfaces.

distribution similarly to the situation in graded-index profiles. However, as we shall see such a hypothesis is not supported by near-field studies.

The electric field  $E$  is constructed by a linear combination of the eigenfields. For a not too narrow linewidth of the light source we may neglect cross-terms in  $|E|^2$  and for uniform launch and attenuation we thus expect to measure an intensity distribution proportional to the average eigenfield intensity, i.e.,  $|E|^2 \approx M^{-1} \sum_m^M |E_m|^2$ . The same will be the case for arbitrary launch and strong inter-modal diffusion. Figure 6 shows the eigenfield intensities with spatial patterns characteristic for a close-to-hexagonal symmetry. The average eigenfield intensity in Panel (B) compares well to the experimentally measured near-field intensity in Panel (C). Together with the DMD measurements this correspondence agrees well with a picture of inter-modal diffusion which tends to populate the modes uniformly.

The eigenmodes fall into different groups with different degeneracies (these degeneracies are slightly lifted due to a weakly broken symmetry in the real fiber) as evident from both the effective index in panel (A) of Fig. 5 as well as the intensity plots (click panel (A) in Fig. 6). The first two eigenmodes ( $m = 1, 2$ ) are the doubly degenerate fundamental mode corresponding to the two polarization states of the fundamental mode in standard fibers and from a practical point of view they can be considered polarization states though the “ $x$ -polarization” in principle has a very small  $y$ -component and vice versa.

For the  $50\ \mu\text{m}$  PCF (see lower right inset of Fig. 1) with  $\text{NA} \simeq 0.05$  we have carried out the same analysis of the effective index and found that  $M = 20$  eigenmodes are guided. Since  $M$  increases with both increasing NA and core size,  $M$  can be low even for a large core as long as the NA is not too high. Figure 7 shows results for the time-delay which as expected has a more narrow distribution compared to the results for the PCF with the  $33\ \mu\text{m}$  core, see panel (B) of Fig. 5. The width  $\Delta T \simeq 0.00054 \times L/c$  corresponds to  $B_T \times L \simeq 559 \text{ MBit/s} \times \text{km}$ . The experimental value is larger by more than 70% which is attributed to inter-modal diffusion.

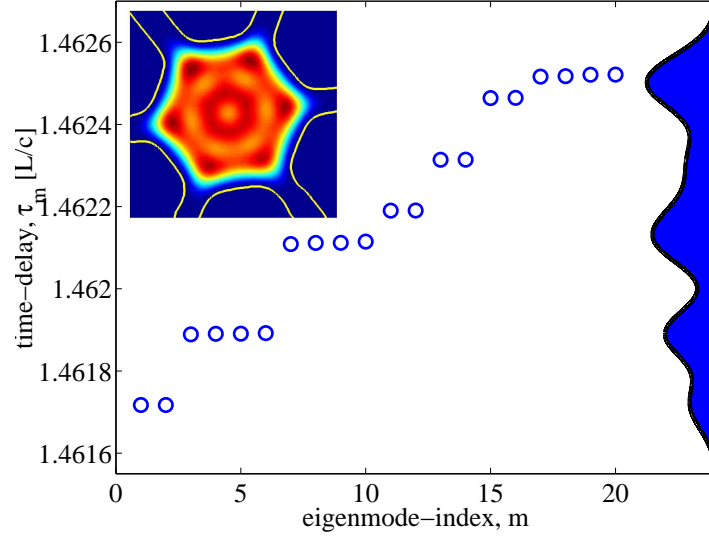


Fig. 7. Time-delays of the  $M = 20$  guided eigenmodes in the  $50\mu\text{m}$  PCF (see lower right inset in Fig. 1). The filled curve shows the distribution  $P(\tau_m)$  and the inset shows the simulated average eigenfield intensity with contour lines indicating the air-silica interfaces.

## 5 Conclusions

For the first time, quasi error-free transmission of 10 Gbit/s digital data signals over a multi-mode photonic crystal fiber with  $50\mu\text{m}$  core diameter and as much as 100 m length has been demonstrated. With some optimizations concerning design and fabrication, these PCFs show good prospects as an alternative to graded-index fibers in optical datacom environments. Comparing to numerical simulations indicates that the high bit-rate may be partly supported by inter-modal diffusion.